ACS Catalysis

Research Article

pubs.acs.org/acscatalysis

Catalytic Transformation of Levulinic Acid to 2-Methyltetrahydrofuran Using Ruthenium–*N*-Triphos Complexes

Andreas Phanopoulos, Andrew J. P. White, Nicholas J. Long,* and Philip W. Miller*

Department of Chemistry, Imperial College London, South Kensington, London, SW7 2AZ, United Kingdom

Supporting Information

ABSTRACT: A series of pre- or in situ-formed ruthenium complexes were assessed for the stepwise catalytic hydrogenation of levulinic acid (LA) to 2-methyltetrahydrofuran (2-MTHF) via γ-valerolactone (γVL) and 1,4-pentanediol (1,4-PDO). Two different catalytic systems based on the branched triphosphine ligands Triphos ($CH_3C(CH_2PPh_2)_3$) and *N*-triphos ($N(CH_2PPh_2)_3$) were investigated. The most active catalyst was the preformed ruthenium species $[RuH_2(PPh_3)\{N(CH_2PPh_2)_3\text{-}\kappa^3P\}]$ (**5**), which gave near quantitative conversion of LA to 1,4-PDO when no acidic additives were present, and 87% 2-MTHF when used in conjunction with $HN(Tf)_2$. Various acidic additives were assessed to promote the final transformation of 1,4-PDO to 2-MTHF; however, only $HN(Tf)_2$ was found to be effective, and NH_4PF_6 and *para*-toluenesulfonic acid (*p*-TsOH) were found to be detrimental. Mechanistic investigations were carried out to explain the observed catalytic trends and importantly showed that PPh_3 dissociation from **5** resulted in its improved catalytic reactivity. The presence of acidic additives removes catalytically necessary hydride ligands and may also compete with the substrate for binding to the catalytic metal center, explaining why only an acid with a noncoordinating conjugate base was effective. Crystals suitable for X-ray diffraction experiments were grown for two complexes: $[Ru(NCMe)_3\{N(CH_2PPh_2)_3\text{-}\kappa^3P\}]$ (**14**) and $[Ru_2(\mu\text{-}Cl)_3\{N(CH_2PPh_2)_3\text{-}\kappa^3P\}_2][BPh_4]$ (**16**).

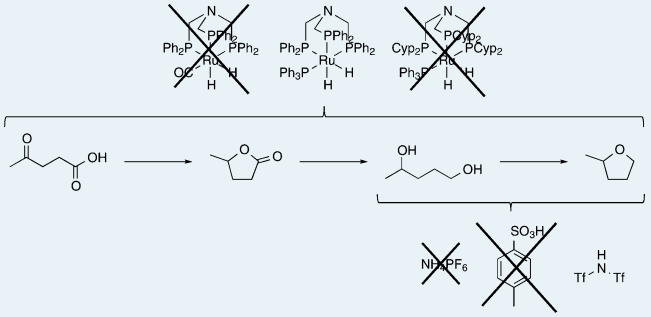

KEYWORDS: *N-triphos, ruthenium, catalysis, levulinic acid, hydrogenation, triphos, 1,4-pentanediol, 2-methyltetrahydrofuran, biomass*

INTRODUCTION

The production of fuels and platform chemicals from materials other than nonrenewable resources is central to achieving a sustainable future. Lignocellulosic biomass represents the largest source of biorenewable carbohydrates and, as such, is a prime candidate for derivatization into other more valuable compounds. Consequently, there has recently been a great deal of academic and industrial interest in its conversion to other products.[1−5] Biomass-derived raw materials in general contain excess functionality, and maintaining only the desired functionality in the final product is key to their successful implementation in upstream industrial and consumer items.[1b,6] In general, these raw materials must undergo a partial deoxygenation process, normally via dehydration reactions, to afford well-defined, so-called platform chemicals. Levulinic acid (LA) is one such platform chemical and can be readily produced during acid treatment of sugar monomers. Initial dehydration of many sugars, such as glucose, fructose, sucrose, etc., affords the cyclic aldehyde 5-hydroxymethylfurfural (5-HMF),[1] a versatile platform chemical in its own right.[7] Under aqueous, acidic conditions, 5-HMF will undergo a ring-opening step to afford levulinic and formic acid (Scheme 1). Starting from a levulinic acid platform, the production of many desirable molecules is possible. Under hydrogenation conditions, LA can be initially transformed into γ-valerolactone (γVL), which has found uses as a biofuel after further esterification,[1e,8] or as a bioderived solvent (Scheme 1).[9] This hydrogenation step has been well-established, and many homogeneous and heterogeneous catalysts have been reported to efficiently and selectively afford γVL.[9,10]

The inherent stability of γVL makes its subsequent transformation difficult and often requires harsh conditions.[6,11] Perhaps most interestingly, a tandem ring-opening/hydrogenation pathway allows the formation of 1,4-pentanediol (1,4-PDO), and a final dehydration affords 2-methyltetrahydrofuran (2-MTHF) (Scheme 1).[6,12] Biogenic diols can be used as monomers to produce high-performance biodegradable polyesters as well as fine-chemical intermediates.[6,13] To an even greater extent than γVL, 2-MTHF has been championed as a bioderived "green" solvent of the future.[14−16] Apart from its sustainable production method, 2-MTHF has several benefits over other ethereal solvents, such as a relatively high boiling point, and immiscibility with water, facilitating workup and recovery.[14]

Recently, several reports have highlighted the use of a tripodal phosphine ligand, the so-called "triphos" scaffold, for

Received: December 16, 2014
Revised: March 7, 2015
Published: March 9, 2015

DOI: 10.1021/cs502025t
ACS Catal. 2015, 5, 2500−2512

Scheme 1. Reaction Sequence for the Transformation of Bioderived Sugar Monomers into Levulinic Acid via 5-Hydroxymethylfurfural, And Subsequent Valorization via Sequential Hydrogenation and Dehydration Reactions To Ultimately Afford 2-Methyltetrahydrofuran

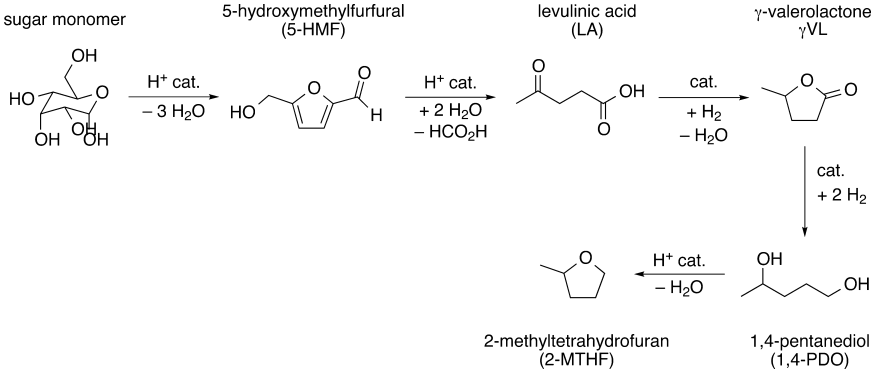

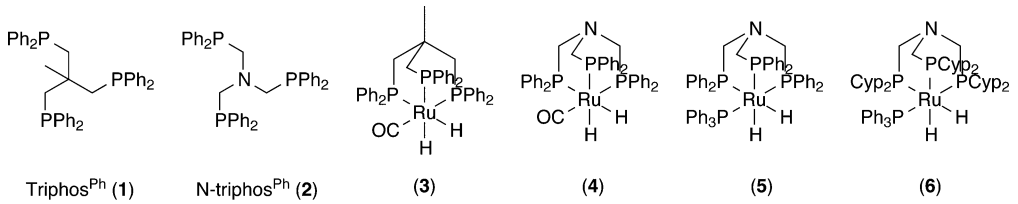

Figure 1. Carbon- and nitrogen-centered triphosphine ligands and their complexes investigated in this work.

Table 1. Screening of Preformed and in-Situ-Generated Complexes for the Catalytic Hydrogenation of Levulinic Acid to 1,4-Pentanediol.[a]

				yield, %[d]			
entry	catalyst	temperature, °C	pressure, bar	γVL	1,4-PDO	2-MTHF	ref
1	Triphos^{Ph}/[Ru(acac)$_3$]	150	65	9	83	0	this work
2[b]	Triphos^{Ph}/[Ru(acac)$_3$]	160	100	3	95	0	12
3	**3**	150	65	85	2	0	this work
4[c]	**3**	160	100	22	73	3	24
5	*N*-triphos^{Ph}/[Ru(acac)$_3$]	150	65	60	37	2	this work
6	**4**	150	65	53	36	<1	this work
7	**5**	150	65	1	99	0	this work
8	**6**	150	65	61	1	1	this work

[a]Conditions: 10 mmol LA, 20 mL THF, 0.5 mol % complex or 0.5 mol % [Ru(acac)$_3$] and 1.0 mol % ligand, reaction time 25 h. [b]10 mmol LA, no solvent, 0.1 mol % [Ru(acac)$_3$], 0.2 mol % Triphos^{Ph}, reaction time 18 h. [c]10 mmol LA, no solvent, 0.1 mol % complex, reaction time 18 h. [d]Yield determined by GC analysis; full conversion was achieved in all cases.

the formation of catalysts for use in conventionally difficult catalytic transformations.[4,12,17−23] The dominance of the triphos ligand is likely to be due to the inherent stability imparted via multidentate coordination of three phosphine arms, preventing or at least slowing catalyst decomposition. The eponymous Triphos^{Ph} ligand (**1**) (Figure 1) has been used in a multicomponent, ruthenium-based system that was found to selectively produce γVL, 1,4-PDO, or 2-MTHF, depending on the conditions used.[12] The use of acidic additives was found to be critical for transforming 1,4-PDO to 2-MTHF, and consequently, a catalytic quantity of H^+ was incorporated into the proposed catalytic mechanism.[24] A similarly tunable heterogeneous system using highly dispersed copper in a zirconia matrix was reported to effectively transform γVL into 1,4-PDO or 2-MTHF if the catalyst was prepared at lower calcination temperatures.[6] Like other heterogeneous catalysts, however, this catalyst requires very high temperatures (>200 °C), decreasing its viability for industrial use.

Herein, we report the use of a relatively unexplored family of nitrogen-centered triphos ligands (Figure 1) for use as homogeneous catalysts for the hydrogenation of levulinic acid. The *N*-triphos ligand differs only from the parent triphos ligand at the central bridgehead atom by replacement of a C−CH_3 with a nitrogen atom. The main advantage of this *N*-triphos ligand system over the carbon-centered analogue is its ease of synthesis and accessibility to a much wider range of phosphine arm substituents.[17a,25−29] In this report, catalysts were generated in situ either from ruthenium(III) precursors or from preformed ruthenium(II) complexes.[29] Mechanistic studies were undertaken to explain the observed product distribution and catalytic activity of these *N*-triphos systems.

RESULTS AND DISCUSSION

Conversion of Levulinic Acid to 1,4-PDO. The hydrogenation of levulinic acid was investigated initially using in situ catalysts formed from [Ru(acac)$_3$] and the diphenylphosphino-containing ligands Triphos^{Ph} (**1**) and *N*-triphos^{Ph} (**2**). The

DOI: 10.1021/cs502025t
ACS Catal. 2015, 5, 2500−2512

Scheme 2. Synthesis of Ruthenium Dihydride Carbonyl Complexes 3 And 4 Under Mild Conditions

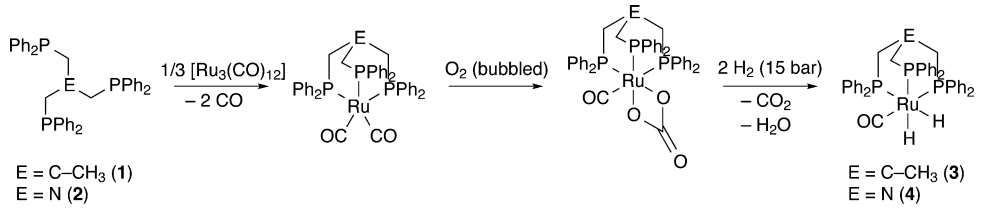

Table 2. Screening of Preformed and in-Situ-Generated Complexes for the Catalytic Hydrogenation of Levulinic Acid to 2-Methyltetrahydrofuran Using Acidic Additives[a]

				yield, %[c]			
entry	catalyst	additive	pressure, bar	γVL	1,4-PDO	2-MTHF	ref
1[b]	Triphos^{Ph}/[Ru(acac)$_3$]	NH_4PF_6	100	8	35	53	12
2[b]	Triphos^{Ph}/[Ru(acac)$_3$]	*p*-TsOH	100	58	1	39	12
3	Triphos^{Ph}/[Ru(acac)$_3$]	NH_4PF_6	65	73	5	2	this work
4	**3**	NH_4PF_6	65	70	2	0	this work
5	*N*-triphos^{Ph}/[Ru(acac)$_3$]	NH_4PF_6	65	60	35	5	this work
6	**4**	NH_4PF_6	65	95	<1	0	this work
7	**4**	*p*-TsOH	65	77	0	0	this work
8	**5**	NH_4PF_6	65	68	8	<1	this work
9	*N*-triphos^{Ph}/[Ru(acac)$_3$]	$HN(Tf)_2$	65	54	0	45	this work
10	**5**	$HN(Tf)_2$	65	10	<1	87	this work

[a]Conditions: 10 mmol LA, 20 mL THF, 0.5 mol % complex or 0.5 mol % [Ru(acac)$_3$] and 1.0 mol % ligand, 5.0 mol % additive, 150 °C, reaction time 25 h. [b]10 mmol LA, no solvent, 0.1 mol % [Ru(acac)$_3$], 0.2 mol % Triphos^{Ph}, 1.0 mol % additive, 160 °C, reaction time 18 h. [c]Yield determined by GC; full conversion was achieved in all cases.

reaction conditions employed, 65 bar and 150 °C, were milder than those of 100 bar and 160 °C previously reported by Lietner et al.[12] In line with the reactivity reported by Leitner et al., when the **1**/[Ru(acac)$_3$] system was used, good conversion to 1,4-PDO was observed (83%), with small amounts of γVL (9%) and no 2-MTHF (Table 1, entry 1). When the ligand was switched to the nitrogen-centered analogue **2**, the product distribution was considerably altered, with γVL being the major product. Interestingly, trace amounts of 2-MTHF were also observed in this reaction (Table 1, entry 5).

Encouraged by these in situ catalytic results, we sought to investigate various well-defined ruthenium complexes. Several reports have highlighted carbonyl dihydride species as being "dormant" forms of the active catalyst during similar reactions;[12,24] hence, such species could provide an excellent precatalyst. Recently, we reported the facile and high-yielding synthetic routes to a series of ruthenium carbonyl dihydride complexes, prepared from *N*-triphos ligands (Scheme 2).[29] We also wished to make comparisons with the previously reported carbonyl dihydride complex featuring Triphos^{Ph} [$RuH_2(CO)$-{$CH_3C(CH_2PPh_2)_3$-κ^3P}] (**3**); however, the reported synthesis proved to be unsatisfactory, involving either several highly air- and moisture-sensitive steps[30,31] or harsh reaction conditions at high temperatures and pressures.[24] Complex **3**, however, could be easily prepared in high yields via the formation of the stable intermediate carbonate complex, followed by a low-pressure hydrogenation to give **3** (Scheme 2).

Complex **3** has previously been tested as a catalyst for the hydrogenation of LA at 100 bar H_2 and 160 °C (Table 1, entry 4),[24] and although it gave poorer yields of 1,4-PDO than the related in-situ-generated system (**1**/[Ru(acac)$_3$]) under the same conditions (Table 1, entry 2),[12] the major product was still found to be 1,4-PDO (73% and 95%, respectively). Interestingly, at the lower pressure and temperature conditions used during this study (65 bar H_2, 150 °C), when **3** was implemented as the catalytic species, formation of γVL was predominant (Table 1, entry 3). This is in contrast to the analogous *N*-triphos^{Ph} complex [$RuH_2(CO)${$N(CH_2PPh_2)_3$-κ^3P}] (**4**), where both the preformed complex (Table 1, entry 6), and in-situ-generated system (Table 1, entry 5) gave similar product distributions. Despite previous reports showing **3** can be isolated from catalytic reaction mixtures of **1**/[Ru(acac)$_3$]/LA,[12] under the conditions used during this study, it appears **3** is not produced from **1**/[Ru(acac)$_3$] mixtures, as evident from the different product distributions. Conversely, the similar product distribution of **4** and **2**/[Ru(acac)$_3$] suggest that the same catalytically active species is produced in both cases for the nitrogen-centered ligands.

Previous reactivity studies of **4** suggested that the carbonyl ligand is robust and will remain coordinated to ruthenium, even under acidic conditions.[29] It was anticipated that by substituting the CO ligand in **4** with a more labile PPh_3 ligand, LA hydrogenation would be more easily facilitated. This hypothesis was based on the mechanism for the catalytic cycle proposed by Leitner et al., which shows that the CO ligand on the complex is replaced by an oxygen bound carbonyl moiety of LA.[24] The triphenylphosphine dihydride complex [$RuH_2(PPh_3)${$N(CH_2PPh_2)_3$-κ^3P}] (**5**) was found to be much more active for the hydrogenation of LA to 1,4-PDO, giving almost quantitative conversion (Table 1, entry 7), thus substantiating this hypothesis.

To probe complex **5** further, the diphenylphosphine groups were exchanged for more bulky and electron-donating dicyclopentylphosphino groups: [$RuH_2(PPh_3)${$N(CH_2PCyp_2)_3$-κ^3P}] (**6**) (Table 1, entry 8). Disappointingly, however, the catalysis did not improve and switched the product distribution back to predominantly γVL. In addition, a greater percentage of products from side reactions was

DOI: 10.1021/cs502025t
ACS Catal. 2015, 5, 2500–2512

observed, consisting mainly of other alcohols. It is uncertain whether these changes are the result of increased steric bulk around the metal center, hindering coordination and activation of the substrate, or due to the ruthenium's being more electron-rich as a result of the donating dialkylphosphines.

Complex **5** is therefore a promising precatalyst for the conversion of LA to 1,4-PDO because it is both air- and moisture-stable in the solid state. Despite the ability of **5** to quantitatively convert LA to 1,4-PDO, further catalytic dehydration of 1,4-PDO to 2-MTHF is also highly desirable. This process requires acidic reaction conditions; hence, catalytic testing was undertaken in the presence of three different proton sources to investigate the formation of 2-MTHF.

Conversion of Levulinic Acid to 2-MTHF. Experiments to convert LA to 2-MTHF were carried out using three different acidic additives, NH_4PF_6, *para*-toluenesulfonic acid (*p*-TsOH) and *bis*(trifluoromethane)sulfonimide ($HN(Tf)_2$), to achieve the desired acidic conditions for this catalytic transformation (Table 2). NH_4PF_6 and *p*-TsOH have previously been implemented by Leitner et al. and displayed moderate to good yields for the production of 2- and 3-MTHF from biomass-derived carboxylic acids (Table 2, entries 1 and 2).[12] It should be noted that previous experiments were conducted under melt conditions (neat LA);[12] however, to ensure good incorporation of H_2 in the present study, a minimum volume of solution was required that necessitated the use of solvent. This was due to limitations in the experimental setup.

In addition, the hydrogenation of amides to amines has been investigated in collaborative work between the groups of Leitner and Cole-Hamilton using ruthenium/Triphos^{Ph} systems with methanesulfonic acid (MSA) as an acidic additive.[18] The role of MSA in these reactions was studied in great detail, and it was found that it acts to remove any hydride ligands as H_2 before coordinating the ruthenium center. Various coordination modes of MSA were found to exist in equilibrium as a mixture of compounds featuring mono- or bidentate MSA as well as bridged dimers. The authors suggest this equilibrium mixture acts as a reservoir for the $[Ru(triphos)]^+$ fragment, which is the entry point for the catalytic cycle.[18]

Using the same adapted conditions that gave excellent yields of 1,4-PDO from LA, the addition of acidic components to the reaction mixture was found to be detrimental to the catalytic process in most cases. Initial comparison of the adapted conditions used during this study with those previously reported using a Triphos^{Ph}/$[Ru(acac)_3]$ catalytic system showed that in the presence of NH_4PF_6, the catalytic cycle was blocked, and almost no 2-MTHF was obtained (Table 2, entry 3). In fact, the acid appeared to significantly alter the catalyst and shift the major product from 1,4-PDO, as was seen in the unacidified experiment (Table 1, entry 1), to γVL. Using preformed catalyst **3**, similar results to the in-situ-generated species were obtained (Table 2, entry 4), suggesting that using either precursor ultimately leads to the same catalytic active species.

Next, the *N*-triphos^{Ph} systems were considered. Unlike the carbon-centered counterparts, a similar product distribution was observed for the *N*-triphos^{Ph}/$[Ru(acac)_3]$ system regardless of whether acidic additives were used (Table 1, entry 5 and Table 2, entry 5). In the absence of acid, the use of either *N*-triphos^{Ph}/$[Ru(acac)_3]$ or **4** as the catalytic system gave similar product distributions, but this was not replicated under acidic conditions. In the presence of NH_4PF_6, a shift to predominantly γVL was observed when **4** was used as the precatalyst (Table 2, entry 6). Here, apparently, different catalytically relevant species are generated. Attempts to increase the yield of 1,4-PDO and push the reaction further along the hydrogenation pathway by varying the amount of acid, pressure, or solvent only proved detrimental (see Supporting Information Table S2).

Increasing the acidity of reaction mixture by using *p*-TsOH instead of NH_4PF_6 again showed no improvement for the production of 1,4-PDO or 2-MTHF (Table 2, entry 7). Similar to the work reported by Cole-Hamilton et al.,[18] *p*-TsOH may be coordinating to the ruthenium under the catalytic conditions and, rather than acting as a reservoir for the catalytically active species, is removing the $[Ru(triphos)]^+$ fragment from the catalytic cycle (vide supra).

The use of complex **5** as the precatalytic species, which gave almost quantitative conversion to 1,4-PDO in the absence of acid, was similarly deactivated in the presence of NH_4PF_6 as **4** (Table 2, entry 8). Clearly, the acidic additive is interacting with the catalyst, resulting in significant catalytic inhibition beyond γVL. Because this same inhibition was not previously observed during similar reactions conducted in neat LA,[12] it is possible that the ability of acidic components to deactivate the catalyst is solvent- or dilution-dependent. Indeed, changing the solvent from THF to dioxane was found to alter the yield of γVL when **4** was used as the precatalyst (Table S2, entry 5).

Finally, the use of a strong acid featuring a highly noncoordinating anion ($HN(Tf)_2$) was evaluated. If the coordination of potentially ligating species formed in situ is responsible for the catalyst inhibition, the removal of this deactivation pathway should increase catalyst efficacy. Gratifyingly, using a *N*-triphos^{Ph}/$[Ru(acac)_3]$ catalytic system in the presence of 5 mol % $HN(Tf)_2$, 2-MTHF was afforded in a 45% yield (Table 2, entry 9). If the product distribution of this catalyst run is compared with the same catalyst system in the absence of acidic components (Table 1, entry 5), similar yields of γVL are observed in both cases. Without an acidic component, the conversion of 1,4-PDO to 2-MTHF cannot be achieved (because this is acid-catalyzed), and consequently, little 2-MTHF was observed in the absence of acidic cocatalysts. With the inclusion of $HN(Tf)_2$, it appears that any 1,4-PDO that is generated is rapidly converted to 2-MTHF without the acid hindering the catalytic activity of the ruthenium complex.

When complex **5** is used in conjunction with $HN(Tf)_2$ as the acidic cocatalyst (Table 2, entry 10), the majority of LA is converted to 2-MTHF (87%), making this catalytic system among the most active for this transformation, and under relatively mild conditions compared with those previously reported.[12,24] Similar to the in-situ-generated catalyst (Table 2, entry 9), $HN(Tf)_2$ does not hinder the activity of the ruthenium species, allowing the transition metal component to convert LA to 1,4-PDO, at which point the acidic component can catalyze the final transformation of 1,4-PDO to 2-MTHF. The different product distributions obtained when various acidic additives are utilized suggest that this additive must be not only highly acidic, but also highly noncoordinating.

The homogeneous nature of the catalyst was implied by mercury poisoning experiments, which demonstrated that elemental mercury did not alter the activity of the catalysts.[32] In addition, upon completion of catalytic runs, if efforts were taken to ensure no oxidative decomposition of any ruthenium species present and the final reaction mixture was subjected to

DOI: 10.1021/cs502025t
ACS Catal. 2015, 5, 2500−2512

fractional distillation to remove catalytic products, well-defined ruthenium complexes were always found to be present. Qualitatively, the reaction mixture maintained a bright orange/red color, indicative of ruthenium–*N*-triphos complexes. If catalyst decomposition to ruthenium nanoparticles or "ruthenium black" had occurred, a significant darkening of the solution would be expected. This color was maintained upon storage of the final reaction mixture in air at −30 °C. Although these ruthenium species could not be fully characterized, their $^{31}P\{^{1}H\}$ NMR spectra indicated ligand coordination was preserved, and under some catalytic conditions, so were ruthenium–hydride moieties.

Mechanistic Investigation. Under our catalytic conditions, the data suggest four main conclusions: (i) in general, systems involving *N*-triphos performed on a par with or better than analogous systems with Triphos for the formation of 1,4-PDO; (ii) the inclusion of NH_4PF_6 or *p*-TsOH suppresses the overall catalytic activity, whereas (iii) inclusion of $HN(Tf)_2$ appears to maintain similar catalytic activity and greatly facilitates the conversion of 1,4-PDO to 2-MTHF; and (iv) increasing the lability of ancillary ligands present on the preformed catalyst precursors increases efficacy. A series of stoichiometric reactions were performed between catalytic species and levulinic acid under various conditions to help explain and enforce some of these observations.

The inclusion of NH_4PF_6 was found to be highly detrimental to catalysis when **3** or **4** was used as the precatalytic species. Consequently, the reactivity of these complexes with LA was studied both in the presence and absence of this proton donor. Work already published by Leitner et al. has investigated the reactivity of **3** and shown that it will react cleanly with LA at room temperature over several hours to form $[RuH\{CH_3C(CH_2PPh_2)_3\}\text{-}\kappa^3P\{CH_3C(O)(CH_2)_2C(O)O\text{-}\kappa^2O\}]$ (**7**).[24] During this reaction, the CO ligand is replaced by a neutral donor carbonyl moiety of LA, and one hydride ligand of **3** will react with the acid moiety of LA, releasing H_2 and enabling coordination of the resultant COO^- group (Scheme 3). This affords a complex with LA bound in a bidentate coordination mode, with one hydride ligand remaining.

Scheme 3. Reaction of Carbonyl Dihydride Complexes 3 and 4 with Levulinic Acid

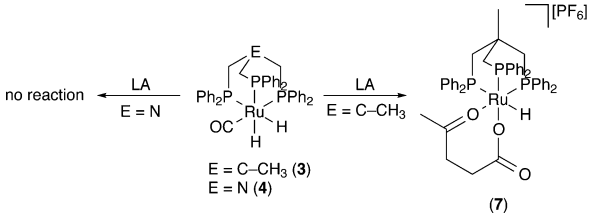

Conversely, an earlier study on **4** by our group shows markedly different reactivity. Complex **4**, which is analogous to **3** except for the inclusion of a nitrogen atom at the apical position of the triphosphine ligand, shows no direct reactivity with LA, even when heated for extended periods.[29] This was surprising to us, considering the structural similarity of the two complexes. Efforts are currently underway within our group to understand this unexpected stability; however, long-range nitrogen–metal interactions (>3.4 Å) may be partially responsible (see Supporting Information). Similar interactions have previously been observed in molybdenum–*N*-triphos^{Ph} complexes.[33]

In the presence of NH_4PF_6 in acetonitrile, both complexes **3** and **4** showed identical reactivity (Scheme 4), releasing hydrogen and forming cationic, solvent-bound complexes **8** and **9**, respectively.[29] The reactivity of **9** with LA has been previously reported by us, during an initial screening of the reactivity of ruthenium complexes featuring **2**, and shows LA coordination can be realized via this route. Similar to the structure of **7**, LA coordination in **9** occurs with loss of a hydride ligand as H_2, with the second coordinating point accessing the metal center through loss of the bound acetonitrile, affording $[Ru(CO)\{N(CH_2PPh_2)_3\}\text{-}\kappa^3P\{CH_3C(O)(CH_2)_2C(O)O\text{-}\kappa^2O\}][PF_6]$ (**11**) (Scheme 4).[29]

Complex **8** featuring the carbon-centered ligand **1** was found to react in a manner identical to **9** in the presence of LA, releasing the bound acetonitrile moiety and the remaining hydride ligand to afford $[Ru(CO)\{CH_3C(CH_2PPh_2)_3\}\text{-}\kappa^3P\{CH_3C(O)(CH_2)_2C(O)O\text{-}\kappa^2O\}][PF_6]$ (**10**) after LA coordination. An NMR-scale reaction between **8** and 1.5 equiv of LA at room temperature showed the three signals corresponding to **8** in its $^{31}P\{^{1}H\}$ NMR spectrum replaced by those of **10** over approximately 10 h (Figure 2). The ^{1}H NMR spectra recorded over the first 10 h of the same reaction show the disappearance of the doublet-of-triplets centered at −6.28 ppm, corresponding to the hydride ligand of **8** (Figure 3). The formation of **10** as the product of the reaction between **8** and LA was further confirmed by the presence of a mass peak at 869.1677 in the high-resolution mass spectrum.

Attempts to isolate and purify **8** resulted in decomposition to a mixture of $[Ru(CO)(NCMe)_2\{CH_3C(CH_2PPh_2)_3\text{-}\kappa^3P\}]$ and $[Ru(NCMe)_3\{CH_3C(CH_2PPh_2)_3\text{-}\kappa^3P\}]$, among other impurities. Consequently, reaction between **8** and LA was performed using an impure sample, as can be observed in Figures 2 and 3, both of which show additional resonances. The resonances corresponding to **8** were identified through similarities to the previously well-characterized analogous **9**.[29] Nonetheless, the impurities present are not thought to have interfered with the conversion of **8** to **10**, because their corresponding resonances remained unaltered throughout the course of the reaction.

An important difference to note between complexes **7** and **11** is the presence of a bound hydride in **7** and none in **11**. Computational studies of the transformation of both LA to γVL and γVL to 1,4-PDO on ruthenium start with the migratory insertion of a bound hydride ligand into a coordinated carbonyl moiety of the target compound.[10a,24] This suggests that for **11** to catalytically turn over, initiation steps that result in formation of a Ru–H species must first occur, and this must proceed via displacement of another ligand. This necessary "activation step" may account for the decrease in catalytic activity when NH_4PF_6 is present in the reaction mixture using **4** as the precatalyst, because **11** is likely to be formed in situ. Similar to mechanistic reactions reported by Cole-Hamilton et al. using MSA as acidic additive,[18] the propensity of complexes featuring a $[Ru(triphos)]^+$ fragment to maintain a catalytic ruthenium–hydride moiety is limited in the presence of acids.

Both NH_4PF_6 and *p*-TsOH form potentially coordinating species upon release of H^+: namely, NH_3 and *p*-TsO^-, respectively. In a closed system that does not allow release of these in-situ-generated species, it is likely that they will compete for coordination to the metal center with the substrate. Indeed, this is observed for MSA, which is structurally similar to *p*-TsOH.[18] When **3** is reacted with NH_4PF_6 in THF, a mixture of products is observed in which either THF (**12**) or NH_3 (**13**) coordinates to the empty site generated by loss of a hydride

DOI: 10.1021/cs502025t
ACS Catal. 2015, 5, 2500–2512

Scheme 4. Reaction of Carbonyl Dihydride Complexes 3 and 4 with NH_4PF_6 in Acetonitrile and Complex 4 with NH_4PF_6 in THF, Plus Subsequent Reaction of the Generated Species (8, 9, 12, and 13) with Levulinic Acid

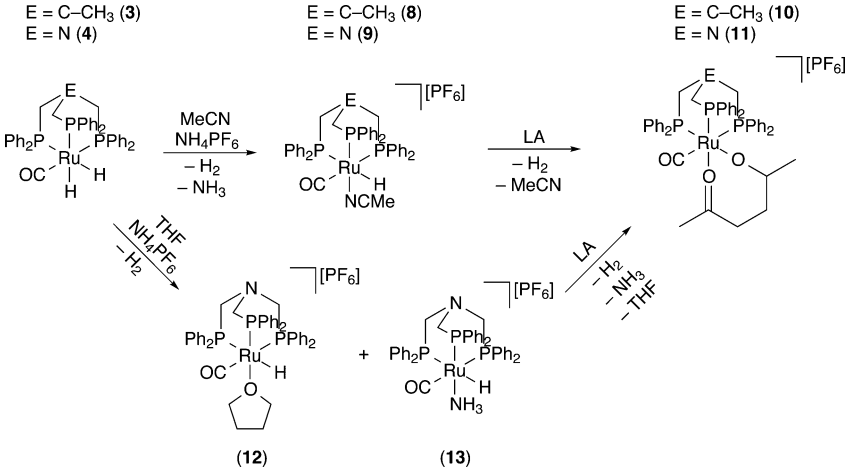

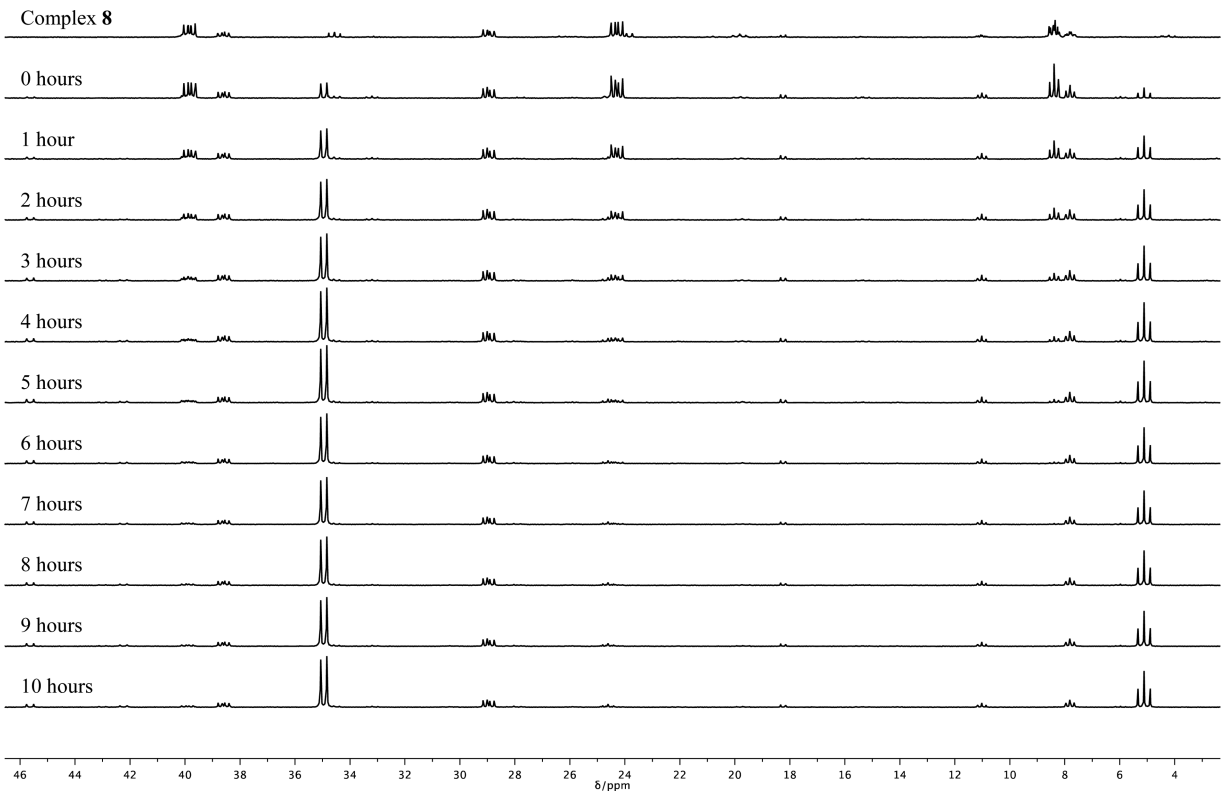

Figure 2. Stacked $^{31}P\{^1H\}$ NMR spectra of reaction between **8** and levulinic acid over 10 h at room temperature (162 MHz, acetone-d_6).

ligand (Scheme 4). Dissolving this reaction mixture in acetonitrile will convert **12** to **9**, demonstrating the greater coordinating ability of acetonitrile over THF, but **13** remains unaffected, suggesting this species is fairly robust. A mass spectrum of this acetonitrile solution shows peaks corresponding to both **9** and **13**.

Acids that generate relatively noncoordinating anions, such as $HN(Tf)_2$, will not compete for metal binding in the same way as NH_4PF_6 or *p*-TsOH, allowing substrate binding to occur more readily. As was observed during the catalytic experiments incorporating acidic additives (Table 2), good conversion of LA to 2-MTHF was observed only when acids with noncoordinating conjugate bases were utilized. Moreover, the coordination of in-situ-generated conjugate bases to the ruthenium center reduced the catalytic activity of this species, changing the major product obtained from 1,4-PDO to γVL.

There is a propensity for complexes **3** and **4** to maintain a coordinated CO ligand, and these complexes were found to underperform compared with **5**, which features a more labile PPh_3 group. Unlike **4**, which displayed no reactivity toward LA,[29] when **5** was reacted directly with LA, free PPh_3 was instantly released at room temperature (◆), and several new species were formed as observed in the $^{31}P\{^1H\}$ NMR spectra (Figure 4). The proportions of these new species changed over the course of 2 weeks at room temperature and after further heating for several hours at 85 °C. Unfortunately, upon working up this reaction solution, only the starting material (complex **5**) was isolated pure, precluding the full character-

DOI: 10.1021/cs502025t
ACS Catal. 2015, 5, 2500–2512

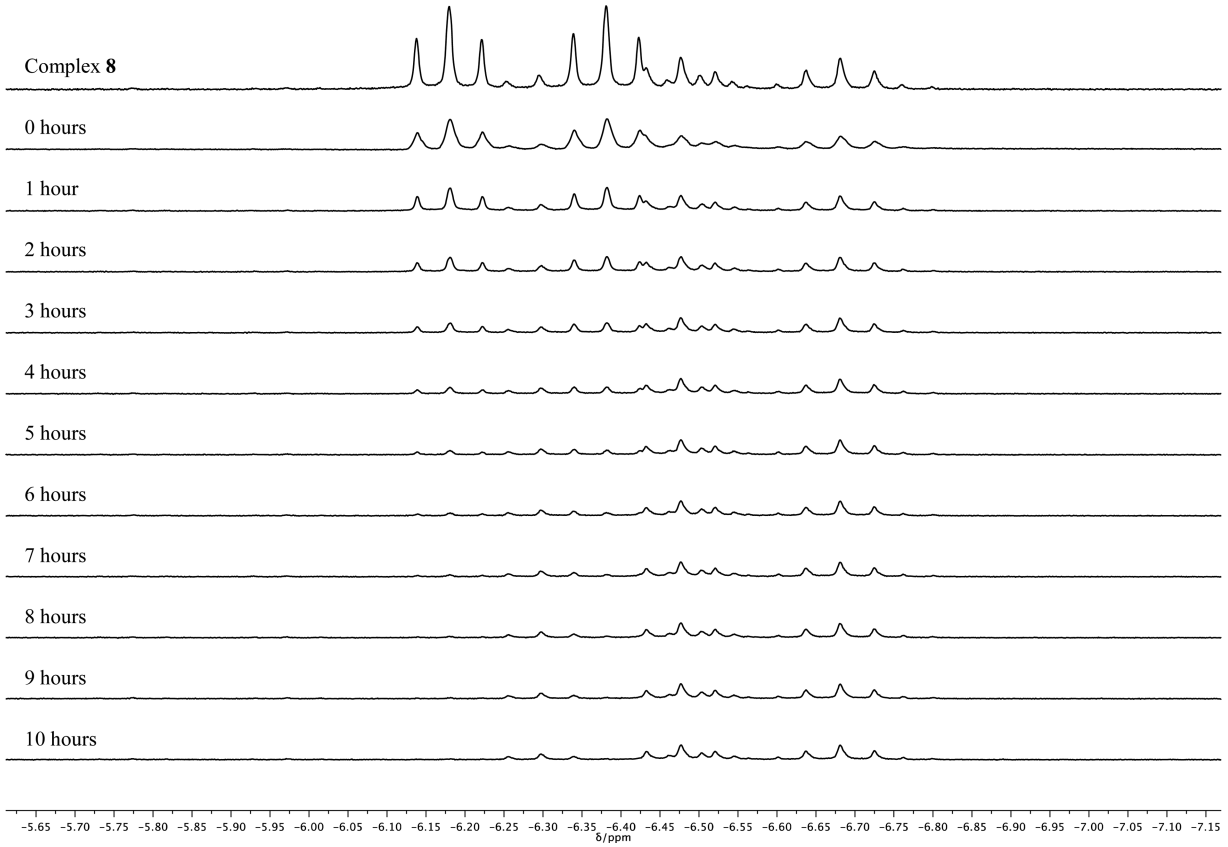

Figure 3. Stacked ^{1}H NMR spectra showing the hydride region of reaction between **8** and levulinic acid over 10 h at room temperature (400 MHz, acetone-d_6).

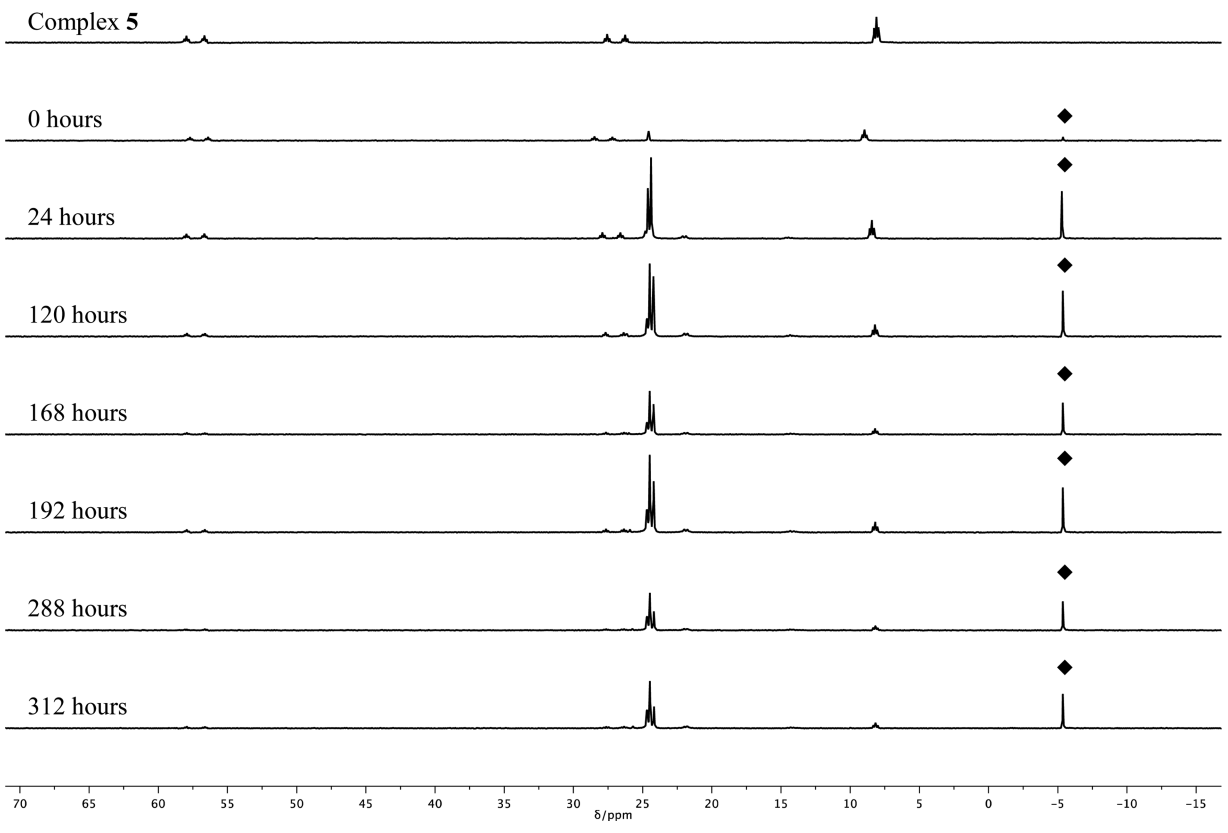

Figure 4. Stacked $^{31}P\{^{1}H\}$ NMR spectra of reaction between **5** and levulinic acid over 13 days at room temperature (162 MHz, C_6D_6). The diamonds (◆) signify the instant release of free PPh_3.

DOI: 10.1021/cs502025t
ACS Catal. 2015, 5, 2500−2512

ization of new species formed during the reaction. Other purification methods gave a mixture of products comprising those observed during the reaction as well as trace amounts of the carbonyl-containing **4**, which presumably formed from the decarbonylation of LA.[24] Despite being unable to satisfactorily characterize the new species, the increased reactivity of **5** over **4** toward LA is evidently due to increased lability of the coordinated ligands due to the immediate loss of PPh_3.

The reactivity of **5** with LA and H_2 in the presence of NH_4PF_6 was investigated, and it also displayed much lower catalytic activity. In contrast to the carbonyl-containing complexes **3** and **4**, when **5** was reacted with NH_4PF_6 in acetonitrile, all of the ligands except for the triphosphine were substituted for solvent, affording $[Ru(NCMe)_3\{N(CH_2PPh_2)_3\text{-}\kappa^3P\}][PF_6]_2$ (**14**) with two PF_6^- units acting as noncoordinating counterions (Scheme 5). This species could be isolated in a

Scheme 5. Synthesis of $[Ru(NCMe)_3\{N(CH_2PPh_2)_3\text{-}\kappa^3P\}][PF_6]_2$ (14) via Two Different Routes

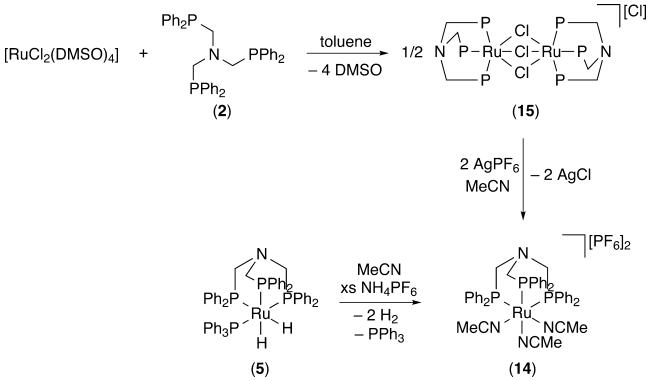

72% yield when 10 equiv of NH_4PF_6 was used. Interestingly, **14** was also exclusively formed when **5** and NH_4PF_6 were reacted in a 1:1 molar ratio and could be isolated in a 49% yield, indicating reaction between the second hydride and NH_4^+ to produce H_2 occurs very rapidly. Crystals suitable for X-ray diffraction analysis were grown by vapor diffusion of diethyl ether into a concentrated acetonitrile solution of **14** overnight. The crystal structure of **14** was found to contain two independent cations (**14-A** and **14-B**, Figures 5 and S22, respectively). The two cations have similar conformations, and in each case, the ruthenium center has a distorted octahedral coordination geometry (Table 3). The tridentate phosphine ligand binds in a facial fashion with P–Ru–P bite angles in the ranges 86.70(4)–91.90(4)° and 87.81(4)–89.73(4)° for complexes **14-A** and **14-B**, respectively. Despite very similar Ru1···N1 separations of 3.468(3) and 3.480(3) Å for **14-A** and **14-B**, respectively, the torsion angles about the Ru1···N1 vectors differ by ∼5°, being ∼58 and 53°, respectively. Both complexes display bond lengths and angles that fall within the standard range of similar complexes.[34]

To produce tangible amounts of **14** for subsequent reactivity studies, it was essential to establish an alternative synthetic procedure for this complex that did not involve **5** as an intermediate. Accordingly, the dimeric species $[Ru_2(\mu\text{-}Cl)_3\{N(CH_2PPh_2)_3\text{-}\kappa^3P\}_2][Cl]$ (**15**) was synthesized from **2** and $[RuCl_2(DMSO)_4]$. This air- and moisture-stable complex precipitated as a yellow powder from toluene and was easily isolated by filtration and subsequent washing to afford an analytically pure sample. Crystals suitable for X-ray diffraction

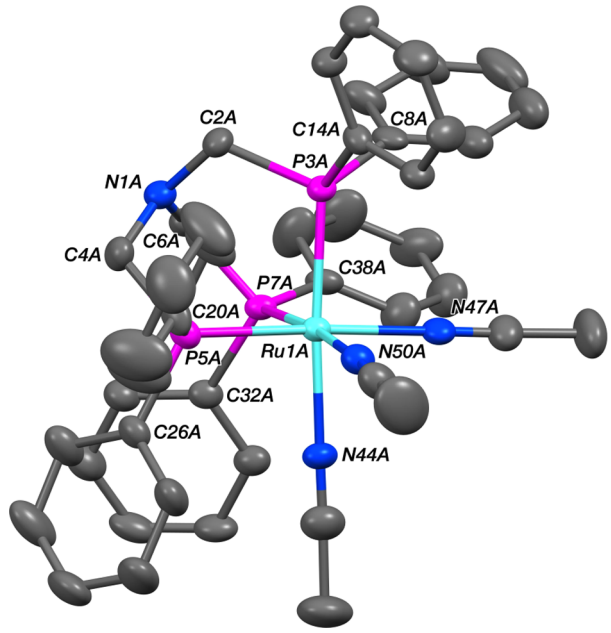

Figure 5. Crystal structure of one (**14-A**) of the two independent complexes present in the crystals of **14** (50% probability ellipsoids).

analysis were obtained first by anion exchange of the chloride counterion to tetraphenylborate (**16**), and grown by slow diffusion of diethyl ether into a methanol solution of **16**. The solid state structure of **16** showed the cation to be the expected diruthenium species with three chloride bridges (Figure 6). Both ruthenium centers have distorted octahedral coordination geometries (Table 4) with the tridentate phosphine ligands occupying facial sites; the P–Ru–P bite angles are in the ranges 86.56(3)–90.73(3)° and 87.96(3)–89.65(3)° at Ru1 and Ru2 respectively). Surprisingly, all three chloride bridges are noticeably asymmetric, with the bond to Ru1 being significantly shorter than that to Ru2 in each case; the Ru–P distances do not show any discernible pattern. The Ru1···N1 separation of 3.444(2) Å is likewise shorter than its Ru2···N51 counterpart (3.512(2) Å), with associated torsional twists about Ru···N vectors of ∼43 and 51°, respectively. The reason for these differing geometries at Ru1 and Ru2 is not readily apparent.

Although it is fairly resistant to chemical transformation, treating **15** with 4 equiv of $AgPF_6$ in acetonitrile under reflux for several hours affords analytically pure **14** after recrystallization from acetonitrile/diethyl ether, with concomitant precipitation of AgCl from the reaction mixture (Scheme 5).

Despite superficially appearing to be reactive due to the potentially labile acetonitrile ligands, **14** is, in fact, robust and stable to both moisture and air in the solid state. Reaction of **14** with 4 bar H_2 at room temperature showed almost no reactivity over a period of 6 days at room temperature, and even extended heating at 50 °C for 7 days resulted in only several new small resonances in the $^{31}P\{^1H\}$ NMR spectrum and no new hydride signals by ^1H NMR spectroscopy, suggesting very slow decomposition rather than formation of a new hydride-containing ruthenium species. The addition of LA to **14** proved similarly unreactive, with almost no reactivity after heating at 50 °C for 7 days. The rapid formation of **14** from **5** suggests that a solvent-bound complex similar to **14** may have formed under the catalytic conditions when **5** is used as a catalytic precursor in the presence of acid. In addition, the stability of **14** in the presence of H_2 and LA suggests that similar species may persist

DOI: 10.1021/cs502025t
ACS Catal. 2015, 5, 2500–2512

Table 3. Selected Bond Lengths (Å) and Angles (deg) for the Two Independent Complexes (14-A and 14-B) Present in Crystals of 14

	A	B		A	B
Ru1−P3	2.3192(11)	2.3149(11)	Ru1−N44	2.107(3)	2.105(3)
Ru1−P5	2.3129(10)	2.3210(11)	Ru1−N47	2.098(3)	2.106(3)
Ru1−P7	2.3271(10)	2.3182(11)	Ru1−N50	2.093(3)	2.101(4)
Ru1···N1	3.468(3)	3.480(3)			
P3−Ru1−P5	91.90(4)	89.12(4)	P5−Ru1−N50	87.82(9)	86.96(10)
P3−Ru1−P7	86.70(4)	87.81(4)	P7−Ru1−N44	91.84(9)	88.35(9)
P3−Ru1−N44	174.91(9)	171.71(9)	P7−Ru1−N47	97.13(9)	99.53(10)
P3−Ru1−N47	90.27(9)	90.14(9)	P7−Ru1−N50	173.93(9)	171.31(10)
P3−Ru1−N50	98.15(10)	100.16(10)	N44−Ru1−N47	85.07(13)	83.25(12)
P5−Ru1−P7	88.37(3)	89.73(4)	N44−Ru1−N50	83.64(12)	84.18(13)
P5−Ru1−N44	92.93(9)	98.21(9)	N47−Ru1−N50	86.54(13)	84.02(13)
P5−Ru1−N47	174.19(10)	170.68(10)			

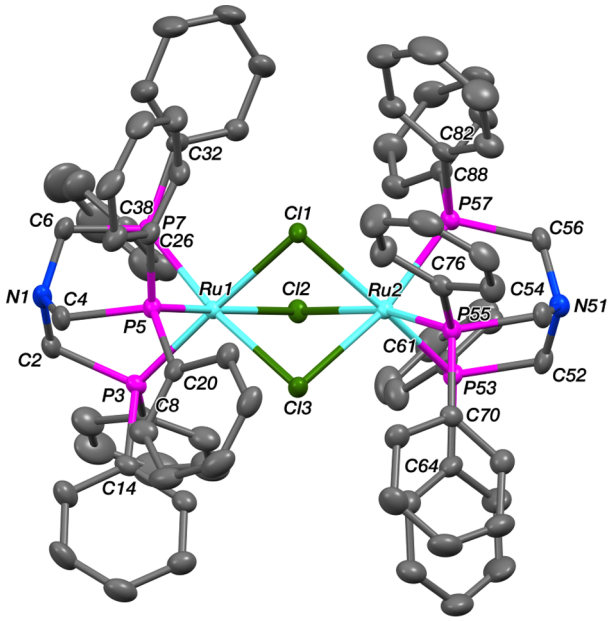

Figure 6. Crystal structure of $[Ru_2(\mu\text{-}Cl)_3\{N(CH_2PPh_2)_3\text{-}\kappa^3P\}_2]\text{-}[BPh_4]$ (**16**) (50% probability ellipsoids).

Table 4. Selected Bond Lengths (Å) and Angles (deg) for 16

Ru1−Cl1	2.4559(6)	Ru2−Cl1	2.4724(6)
Ru1−Cl2	2.4808(7)	Ru2−Cl2	2.5231(7)
Ru1−Cl3	2.4803(7)	Ru2−Cl3	2.4954(7)
Ru1−P3	2.3017(7)	Ru2−P53	2.2701(7)
Ru1−P5	2.2802(7)	Ru2−P55	2.2779(7)
Ru1−P7	2.2712(7)	Ru2−P57	2.2852(7)
Ru1···N1	3.444(2)	Ru2···N51	3.512(2)
Ru1···Ru2	3.4486(3)		
Cl1−Ru1−Cl2	77.58(2)	Cl1−Ru2−Cl2	76.50(2)
Cl1−Ru1−Cl3	77.70(2)	Cl1−Ru2−Cl3	77.11(2)
Cl1−Ru1−P3	177.99(3)	P53−Ru2−Cl1	166.61(3)
Cl1−Ru1−P5	93.65(2)	P55−Ru2−Cl1	105.32(2)
Cl1−Ru1−P7	95.21(2)	P57−Ru2−Cl1	89.15(2)
Cl2−Ru1−Cl3	77.51(2)	Cl3−Ru2−Cl2	76.46(2)
Cl2−Ru1−P3	101.30(2)	P53−Ru2−Cl2	90.95(2)
Cl2−Ru1−P5	169.03(2)	P55−Ru2−Cl2	167.04(3)
Cl2−Ru1−P7	96.57(2)	P57−Ru2−Cl2	104.95(2)
Cl3−Ru1−P3	100.46(2)	P53−Ru2−Cl3	104.76(3)
Cl3−Ru1−P5	94.31(2)	P55−Ru2−Cl3	91.32(2)
Cl3−Ru1−P7	171.53(2)	P57−Ru2−Cl3	165.54(3)
P5−Ru1−P3	87.26(3)	P53−Ru2−P55	87.96(3)
P3−Ru1−P7	86.56(3)	P53−Ru2−P57	89.65(3)
P5−Ru1−P7	90.73(3)	P55−Ru2−P57	87.97(3)
Ru1−Cl1−Ru2	88.81(2)	Ru1−Cl3−Ru2	87.75(2)
Ru1−Cl2−Ru2	87.13(2)		

in the catalytic reaction mixture and may represent a significant pathway for potentially complete catalyst deactivation, or at the least temporary removal from the catalytic cycle. The identification of complexes **8**−**14** and their observed high stability and low reactivity suggest that these species are being formed under catalytic conditions and are responsible for the low catalyst activity when NH_4PF_6 is included as a catalytic additive.

CONCLUDING REMARKS

The sequential catalytic hydrogenation of the biomass-derived compound levulinic acid (LA) to γ-valerolactone (γVL); 1,4-pentanediol (1,4-PDO); and, ultimately, 2-methyltetrahydrofuran (2-MTHF) using a series of *N*-triphos−ruthenium complexes as catalytic precursors has been investigated. Previously, the ruthenium dihydride complex $[RuH_2(CO)\{CH_3C(CH_2PPh_2)_3\text{-}\kappa^3P\}]$ (**3**) had been identified as a dormant form of the active catalyst for the hydrogenation of LA, and the analogous complex featuring the nitrogen-centered triphosphine ligand **2**, $[RuH_2(CO)\{N(CH_2PPh_2)_3\text{-}\kappa^3P\}]$ (**4**), was found to perform better under the relatively mild conditions used during this study. Increasing the overall lability of catalyst by substitution of the carbonyl ligand in **4** with a PPh_3 ligand afforded a complex that, when used as a catalyst precursor, allowed almost quantitative conversion of LA to 1,4-PDO under relatively mild conditions.

The use of acidic additives was found to be detrimental to catalysis in two cases (NH_4PF_6 and *p*-TsOH), whether a preformed complex was used or an in-situ-generated system. The only system to maintain similar catalytic activity under both non- and acidified conditions was $N\text{-triphos}^{Ph}/[Ru(acac)_3]$. Changes to the reaction condition,s including varying the amount of acidic additive, higher pressures, or different solvents, did not lead to enhanced generation of 2-MTHF but, in most cases, led to increased side-product formation. Using the strong, noncoordinating acid $HN(Tf)_2$ was found to considerably enhance conversion of LA to 2-MTHF, in the best case leading to yields of 87%. This is likely due to the noncoordinating nature of the conjugate base, which will not compete with the substrate for binding to the metal center.

DOI: 10.1021/cs502025t
ACS Catal. 2015, 5, 2500−2512

Mechanistic investigations were conducted to try to identify possible species that would be present and potentially persistent under the catalytic conditions. Carbon-centered Triphos^{Ph} was found to show activity different from that of associated *N*-triphos^{Ph} systems, as demonstrated by the reactivity between **3** or **4** and LA,[29] and may account for the differing product distributions observed when these complexes are used catalytically. Reaction of **3** and **4** with 1 or more equivalents of NH_4PF_6 in MeCN solvent resulted in loss of a single hydride ligand, lost as H_2, and coordination of acetonitrile solvent. These intermediary complexes were found to react with LA through dissociation of the remaining hydride moiety and the bound solvent molecule, allowing LA to coordinate in a bidentate fashion. Importantly it seems, upon LA coordination under acidic conditions, no hydride ligands remain coordinated. Because migratory insertion of a hydride has been suggested as the first step in the catalytic hydrogenation of LA,[24] the lack of hydrides under acidic conditions is likely to hinder catalysis.

The inclusion of more-labile ancillary ligands to the complexes being used as precatalytic species resulted in better catalytic activity, with **5** giving almost quantitative conversion of LA to 1,4-PDO. This increased reactivity is evident from the reaction between **5** and LA, which forms several unidentified products; however, it importantly shows instantaneous release of PPh_3. This indicates that the lability of this ligand is integral for its catalytic activity. Upon treatment of **5** with NH_4PF_6, all ancillary ligands are lost and substituted for acetonitrile solvent, forming the highly stable dicationic complex **12**. Heating this complex in the presence of LA or 4 bar H_2 gave almost no reaction over 7 days and, consequently, may represent a temporary or permanent deactivation pathway if present in the catalytic reaction mixture, which is likely in the presence of NH_4PF_6.

EXPERIMENTAL SECTION

Safety Warning. Experiments with compressed gases must be carried out with appropriate equipment and under rigorous safety precautions.

General Considerations. All preparations were carried out using standard Schlenk line techniques under an inert atmosphere of N_2 unless otherwise stated. Solvents were dried over standard drying agents and stored over 3 Å molecular sieves. All starting materials were of reagent grade and purchased from either Sigma-Aldrich Chemical Co. or VWR International and used without further purification. Triphos^{Ph} (**1**) was purchased from Sigma-Aldrich Chemical Co., and used without further purification. Ligand **2**, *N*-triphos^{Cyp}, and complexes **4**−**6** and $[RuCl_2(DMSO)_4]$ were prepared as previously reported.[24,29,35] Catalytic reactions were performed in a high-pressure adapted Autoclave Engineers 100 mL Mini Reactor with a Universal Reactor Controller Series control unit. Conversion and selectivity of the catalytic reactions were determined via gas chromatography using a Hewlitt Packard Gas Chromatograph 5890 Series II with a J&W Scientific Agilent 122-5032 DB-5 column and equipped with a flame ionization detector (FID) and dodecane as internal standard. Peaks were assigned via GC/MS and pure substance calibration. ^{1}H, ^{13}C{^{1}H}, and ^{31}P{^{1}H} NMR spectra were recorded on Bruker AV-400, AV-500, or DRX-400 spectrometers at 294 K unless otherwise stated. Chemical shifts are reported in parts per million using the residual proton impurities in the solvents for ^{1}H NMR spectroscopy, the solvent for ^{13}C{^{1}H} NMR spectroscopy, and an external H_3PO_4 standard for ^{31}P{^{1}H} NMR spectroscopy. Pseudo doublets, triplets, and doublets-of-triplets that occur as a result of identical *J* value coupling to two or more chemically nonequivalent nuclei are assigned as dd or ddd and are recognized by the inclusion of only one or two *J*-coupling values. ^{13}C{^{1}H} NMR spectra were assigned with the aid of DEPT-135, HSQC, and HMBC correlation experiments. Mass spectrometry analyses were conducted by the Mass Spectrometry Service, Imperial College London. Elemental analyses were carried out by Mr. Stephen Boyer of the School of Human Sciences, London Metropolitan University. X-ray diffraction analyses were carried out by Dr. Andrew White of the Department of Chemistry at Imperial College London. Details of single-crystal X-ray diffraction analysis can be found in the Supporting Information.

General Catalytic Procedure. *Method A.* A solution of levulinic acid (1.16 g, 10.0 mmol); $[Ru(acac)_3]$ (19.8 mg, 0.05 mmol, 0.5 mol %); and triphosphine ligand (1.0 mol %); and, where applicable, acidic additive (5.0 mol %) in THF (20 mL) was syringed into a prepurged high pressure reactor under a flow of nitrogen. The atmosphere was changed to hydrogen by repeatedly pressurizing to 5 bar and depressurizing (×3), before the pressure was raised to 50 bar and the reactor was sealed. The reactor was heated to 150 °C and stirred, causing the internal pressure to rise to 65 bar once the reaction temperature was reached. The reaction mixture was stirred at this temperature and pressure for 25 h before the vessel was cooled in an ice bath and slowly depressurized. The product mixture was analyzed by GC and ^{1}H and ^{31}P{^{1}H} NMR spectroscopy.

Method B. Identical to method A, except a preformed ruthenium catalyst precursor was utilized (0.5 mol %) instead of a $[Ru(acac)_3]$/triphosphine ligand mixture. Analysis of each run was done by GC and ^{1}H and ^{31}P{^{1}H} NMR spectroscopy.

Mercury Poisoning Experiment. A solution of levulinic acid (1.16 g, 10.0 mmol), $[Ru(acac)_3]$ (19.8 mg, 0.05 mmol, 0.5 mol %) and *N*-triphos^{Ph} (61.2 mg, 0.10 mmol, 1.0 mol %) in THF (20 mL) was added via syringe into a prepurged high-pressure reactor under a flow of nitrogen. The atmosphere was changed to hydrogen by repeatedly pressurizing to 5 bar and depressurizing (×3) before the pressure was raised to 50 bar and the reactor was sealed. The reactor was heated to 150 °C and stirred, causing the internal pressure to rise to 65 bar. The reaction mixture was stirred at this temperature and pressure for 2 h before the vessel was cooled in an ice bath and slowly depressuzied. A sample was submitted for GC analysis (Table S1, entry 1). The reaction mixture was transferred to a Schlenk flask, and mercury (200 mg, 1.00 mmol) was added. After stirring for 2 h at room temperature, the mercury was separated from the solution. The solution was transferred back into the high-pressure reactor and repressurized to 50 bar H_2 and heated to 150 °C for 4 h, after which the reactor was cooled in an ice bath and slowly depressurized. A sample was analyzed by GC (Table S1, entry 2). A control experiment was conducted using the same procedure without addition of mercury (Table S1, entries 3 and 4).

Synthesis of $[RuH_2(CO)\{CH_3C(CH_2PPh_2)_3$-$\kappa^3P\}]$ (3). A solution of $[Ru(CO_3)(CO)\{CH_3C(CH_2PPh_2)_3$-$\kappa^3P\}]$ (621 mg, 0.76 mmol) in THF (20 mL) was injected into a high-pressure reactor under a flow of nitrogen. The atmosphere was changed to hydrogen and pressurized to 15 bar at room temperature before the mixture was heated to 100 °C (increasing the

DOI: 10.1021/cs502025t
ACS Catal. 2015, 5, 2500−2512

internal pressure to ∼20 bar) and stirred for 2 h. After the mixture was cooled to room temperature, the gas was carefully vented, and the atmosphere was changed to nitrogen. The solution was transferred from the reactor to a Schlenk flask, filtered, and diluted with ethanol (15 mL), and the solution was concentrated to ∼5 mL, causing precipitation of an orange powder. Additional ethanol (15 mL) was added to fully precipitate the product that was isolated by cannula filtration, washed with ethanol (3 × 3 mL) and dried in vacuo. Complex **3** was isolated as an orange powder (379 mg, 0.50 mmol, 66%) with characterization identical to that previously reported.[24]

NMR-Scale Reaction of [$RuH_2(CO)\{CH_3C(CH_2PPh_2)_3$-$\kappa^3P\}$] (3), NH_4PF_6 and Levulinic Acid. To a Schlenk flask was added [$RuH_2(CO)\{CH_3C(CH_2PPh_2)_3$-$\kappa^3P\}$] (31.7 mg, 0.042 mmol) and suspended in acetonitrile (2 mL). A solution of NH_4PF_6 (6.8 mg, 0.042 mmol) in acetonitrile (1 mL) was added via cannula, and the mixture was stirred at room temperature for 2 h, turning homogeneous. The solvent was removed in vacuo, affording a yellow powder that was dried in vacuo for 15 min, washed with hexane (3 × 2 mL), and again dried in vacuo for 15 min. The powder was then dissolved in acetone-d_6 (0.3 mL) and transferred in its entirety to a Young's tap NMR tube via cannula, which was washed through with additional acetone-d_6 (0.3 mL). Initial NMR analysis was performed on [$RuH(CO)(NCMe)\{CH_3C(CH_2PPh_2)_3$-$\kappa^3P\}$]-[$PF_6$] (**8**): ^{1}H NMR (acetone-d_6, 400 MHz) δ: −6.28 (ddd, 1H, $^2J_{HP}$ = 81 Hz, $^2J_{HP}$ = 16 Hz, Ru−H). $^{31}P\{^1H\}$ NMR (acetone-d_6, 162 MHz) δ: −144.0 (septet, 1P, $^1J_{PF}$ = 706 Hz), 8.0−8.5 (m, 1P), 24.5 (dd, 1P, $^2J_{PP}$ = 43 Hz, $^2J_{PP}$ = 26 Hz), 40.0 (dd, 1P, $^2J_{PP}$ = 43 Hz, $^2J_{PP}$ = 26 Hz). In a separate Schlenk flask was prepared a solution of levulinic acid (7.5 mg, 0.065 mmol, 1.5 equiv) in acetone-d_6 (0.3 mL), and this was added to the NMR tube via syringe. The NMR tube was sealed, stirred for 30 s using a vortex stirrer, and analyzed by ^{1}H and $^{31}P\{^1H\}$ NMR spectroscopy every hour for 10 h. Quantitative conversion of **8** to [$Ru(CO)\{CH_3C(CH_2PPh_2)_3\}$-$\kappa^3P\{CH_3C(O)(CH_2)_2C(O)O$-$\kappa^2O\}$][$PF_6$] (**10**) was observed. ^{1}H NMR (acetone-d_6, 400 MHz) δ: 1.96−1.99 (m, 3H, $CH_3^{Triphos}$), 2.03−2.08 (m, 6H, $CH_2^{Triphos}$), 2.24 (s, CH_3^{LA}), 2.65 (t, $^3J_{HH}$ = 7 Hz, CH_2^{LA}), 2.80 (t, $^3J_{HH}$ = 6 Hz, CH_2^{LA}), 6.99−7.76 (m, 30H, Ph). $^{13}C\{^1H\}$ NMR (acetone-d_6, 127 MHz) δ: 28.1 (s, CH_3^{LA}), 31.5 (m, $CH_2^{Triphos}$), 37.5 (s, CH_2^{LA}), 38.2 (s, CH_2^{LA}), 39.4 (s, $C^{Triphos}$), 129.2 (d, J_{CP} = 11 Hz, CH^{Ph}), 129.8 (dt, J_{CP} = 14 Hz, J_{CP} = 5.5 Hz, CH^{Ph}), 131.2 (s, CH^{Ph}), 131.4 (s, CH^{Ph}), 131.6 (t, J_{CP} = 5 Hz, CH^{Ph}), 132.03 (s, CH^{Ph}), 174.0 (s, CO^{LA}), 191.62 (s, CO^{LA}), 206.9 (s, $CO^{Triphos}$). $^{31}P\{^1H\}$ NMR (acetone-d_6, 162 MHz) δ: −144.0 (septet, 1P, $^1J_{PF}$ = 706 Hz), 5.0 (dd, 1P, $^2J_{PP}$ = 35 Hz), 35.0 (dd, 1P, $^2J_{PP}$ = 35 Hz). HRMS (ES): m/z calcd. for $C_{47}H_{46}O_4P_3{}^{102}Ru$ ([M − PF_6]$^+$) 869.1652, found 869.1677.

NMR-Scale Reaction of [$RuH_2(CO)\{N(CH_2PPh_2)_3$-$\kappa^3P\}$] (4) and NH_4PF_6 in THF. To a Young's tap NMR tube was added [$RuH_2(CO)\{N(CH_2PPh_2)_3$-$\kappa^3P\}$] (33.6 mg, 0.0452 mmol) and NH_4PF_6 (7.7 mg, 0.0472 mmol) dissolved in THF-d_8 (0.7 mL). The NMR tube was shaken for 1 min using a vortex stirrer and analyzed by ^{1}H and $^{31}P\{^1H\}$ NMR spectroscopy over the course of 3 days at room temperature. The formation of two species was observed: [RuH(CO)-(THF)$\{N(CH_2PPh_2)_3$-$\kappa^3P\}$] (**12**) and [$RuH(CO)(NH_3)\{N$-$(CH_2PPh_2)_3$-$\kappa^3P\}$] (**13**). After 3 days, the solvent and volatiles were removed in vacuo, and the resultant powder was redissolved in CD_3CN and analyzed by ^{1}H and $^{31}P\{^1H\}$ NMR spectroscopy and high-resolution mass spectrometry. **12**: $^{31}P\{^1H\}$ NMR (THF-d_8, 162 MHz) δ: −144.0 (septet, 1P, $^1J_{PF}$ = 706 Hz), −13.0 (ddd, 1P, $^2J_{PP}$ = 206 Hz, $^2J_{PP}$ = 26 Hz, $^2J_{PP}$ = 24 Hz), 7.0−8.0 (m, 1P), 25.5−26.0 (m, 1P). **13**: $^{31}P\{^1H\}$ NMR (THF-d_8, 162 MHz) δ: −144.0 (septet, 1P, $^1J_{PF}$ = 706 Hz), −8.5 (dd, 1P, $^2J_{PP}$ = 28 Hz, $^2J_{PP}$ = 23 Hz), 7.0−8.0 (m, 1P), 26.0 (dd, 1P, $^2J_{PP}$ = 34 Hz, $^2J_{PP}$ = 23 Hz). HRMS (ES): m/z calcd. for $C_{40}H_{40}N_2OP_3{}^{102}Ru$ ([M − PF_6]$^+$) 759.1397, found 756.7177. Attempts to purify and isolate these species resulted in decomposition; however, direct reaction of a mixture of **12** and **13** with levulinic acid resulted in formation of [Ru(CO)-$\{N(CH_2PPh_2)_3\}$-$\kappa^3P\{CH_3C(O)(CH_2)_2C(O)O$-$\kappa^2O\}$][$PF_6$] (**11**) with characterization identical to what has previously been reported.[29]

NMR-Scale Reaction of [$RuH_2(PPh_3)\{N(CH_2PPh_2)_3$-$\kappa^3P\}$] (5) and Levulinic Acid. To a Young's tap NMR tube was added [$RuH_2(PPh_3)\{N(CH_2PPh_2)_3$-$\kappa^3P\}$] (16.1 mg, 0.017 mmol) dissolved in C_6D_6 (0.7 mL); initial NMR analysis were performed. In a separate Schlenk flask was prepared a solution of levulinic acid (56.3 mg, 0.48 mmol) in C_6D_6 (2 mL)., and 0.1 mL (0.024 mmol LA, 1.5 equiv) was added to the NMR tube via syringe. The NMR tube was sealed and analyzed by NMR spectroscopy regularly over the course of 2 weeks at room temperature. The NMR tube was then heated to 85 °C for a total of 35 h, with analysis by NMR spectroscopy at room temperature periodically. Removal of the solvent in vacuo and subsequent redissolution of the resultant yellow powder in methanol (2 mL) gave crystals of pure [$RuH_2(PPh_3)\{N$-$(CH_2PPh_2)_3$-$\kappa^3P\}$] when left to stand overnight. The supernatant was saved, and the solvent was removed in vacuo. NMR analysis of the resultant residue in C_6D_6 displayed an uncharacterizable mixture of products, including [$RuH_2(CO)$-$\{N(CH_2PPh_2)_3$-$\kappa^3P\}$] (**4**).

Synthesis of [$Ru(NCMe)_3\{N(CH_2PPh_2)_3$-$\kappa^3P\}$][$PF_6$]$_2$ (12). *Method A.* To a Schlenk flask was added [$RuH_2(PPh_3)\{N$-$(CH_2PPh_2)_3$-$\kappa^3P\}$] (82.1 mg, 0.084 mmol) and NH_4PF_6 (24.6 mg, 0.15 mmol), and the flask was evacuated and backfilled with nitrogen (×3). Acetonitrile (2 mL) was added, and the mixture was stirred at room temperature for 20 h. The solvent was removed in vacuo, and the resultant powder was washed with diethyl ether (3 × 2 mL) and dried in vacuo. Redissolving in acetonitrile and slow diffusion of diethyl ether into the solution by vapor diffusion afforded crystals overnight, which were isolated by cannula filter, washed with diethyl ether (3 × 2 mL), and dried in vacuo. The combined supernatant and washings afforded a second batch of crystals that were isolated and washed as the first batch were. Both batches gave analytically pure white crystals of **12** that were suitable for X-ray diffraction experiments (61.6 mg, 0.055 mmol, 72%). ^{1}H NMR (CD_2Cl_2, 400 MHz) δ: 2.32 (S, 9H, CH_3), 4.23 (s, 6H, CH_2), 7.15−7.28 (m, 24H, CH), 7.30−7.41 (m, 6H, CH). $^{13}C\{^1H\}$ NMR (CD_2Cl_2, 101 MHz) δ: 4.18 (s, CH_3), 50.8−51.1 (m, CH_2), 129.4−129.5 (m, CH), 131.4 (s, CH), 132.3−132.4 (m, CH). $^{31}P\{^1H\}$ NMR (CD_2Cl_2, 162 MHz) δ: 9.0 (s, 3P, PPh_2), −144.0 (heptet, 2P, $^1J_{PF}$ = 712 Hz, PF_6). ^{19}F NMR (CD_2Cl_2, 381 MHz) δ: −72.4 (d, 12F, $^1J_{FP}$ = 712 Hz, PF_6). HRMS (ES): m/z calcd. for $C_{45}H_{45}N_4P_3{}^{102}Ru$ ([M − 2PF_6]$^{2+}$) 418.0950, found 418.0950. Anal. Calcd for $C_{45}H_{45}N_4P_5F_{12}Ru$ (found): C, 48.01 (47.89); H, 4.03 (3.94); N, 4.98 (4.88).

Method B. To a Schlenk flask was added [$Ru_2(\mu$-Cl)$_3\{N$-$(CH_2PPh_2)_3$-$\kappa^3P\}_2$] (146 mg, 0.11 mmol), $AgPF_6$ (114 mg, 0.45 mmol, 4.2 equiv), and acetonitrile (5 mL). The suspension was stirred and heated to 70 °C for 15 h and remained a yellow suspension throughout. After cooling to room temperature and

DOI: 10.1021/cs502025t
ACS Catal. 2015, 5, 2500−2512

allowing to settle, the supernatant was isolated from the powder via cannula filter, and the powder was washed with acetonitrile (2 mL) which was added to the saved supernatant. This solution was concentrated in vacuo to ∼1.5 mL, and the product crystallized by the slow addition of diethyl ether via vapor diffusion. Analytically pure colorless crystals with characterization identical to those obtained via method A (100 mg, 0.089 mmol, 83%) grew overnight.

Synthesis of $[Ru_2(\mu\text{-}Cl)_3\{N(CH_2PPh_2)_3\text{-}\kappa^3P\}_2][Cl]$ (13). To a Schlenk flask was added $[RuCl_2(DMSO)_4]$ (480 mg, 1.00 mmol), **2** (611 mg, 1.00 mmol), and toluene (10 mL), and the mixture was heated to 100 °C for 12 h. Upon heating, the reaction mixture changed to a deep orange color and formed a yellow precipitate. The yellow precipitate was isolated by filtration and washed first with toluene (3 × 15 mL) and then diethyl ether (3 × 15 mL). The light yellow solid was dried in vacuo (760 mg, 0.49 mmol, 97%). ^{1}H NMR (CD_2Cl_2, 400 MHz) δ: 4.09 (br s, 12H, CH_2), 6.88 (t, 24H, $^3J_{HH}$ = 8 Hz, $CH^{Ph\text{-}ortho}$), 7.19 (t, 12H, $^3J_{HH}$ = 8 Hz, $CH^{Ph\text{-}para}$), 7.35 (m, 24H, $CH^{Ph\text{-}meta}$). $^{13}C\{^1H\}$ NMR (CD_2Cl_2, 101 MHz) δ: 53.7 (s, CH_2), 128.0 (s, $CH^{Ph\text{-}ortho}$), 129.9 (s, $CH^{Ph\text{-}para}$), 133.8 ($CH^{Ph\text{-}meta}$). $^{31}P\{^1H\}$ NMR (CD_2Cl_2, 162 MHz) δ: 18.0 (s). HRMS (ES): m/z calcd. for $C_{78}H_{72}N_2P_6Cl_3{}^{102}Ru_2$ ($[M - Cl]^+$) 1531.1274, found 1531.1310. Anal. Calcd for $C_{78}H_{72}N_2P_6Cl_4Ru_2.CH_2Cl_2$ (found): C, 57.43 (57.76); H, 4.51 (4.67); N, 1.70 (1.62).

Synthesis of $[Ru_2(\mu\text{-}Cl)_3\{N(CH_2PPh_2)_3\text{-}\kappa^3P\}_2][BPh_4]$ (14). To a solution of **13** (200 mg, 0.13 mmol) in dichloromethane (5 mL) was slowly added a solution of $NaBPh_4$ (44.5 mg, 0.13 mmol) in acetonitrile (0.5 mL), and the mixture was stirred at room temperature for 2 h. A light colored precipitate of NaCl formed over this time. The yellow filtrate was collected by filtering through a small pad of Celite. Crystals suitable for X-ray diffraction experiments were obtained overnight by slow diffusion of diethyl ether into this solution and were collected as yellow crystals after isolation and washing with diethyl ether (146 mg, 0.079 mmol, 62%). ^{1}H NMR (CD_2Cl_2, 400 MHz) δ: 4.07 (br s, 12H, CH_2), 6.85 (t, $^3J_{HH}$ = 1 Hz, $CH^{BPh\text{-}para}$), 6.87 (t, 28H, $^3J_{HH}$ = 7 Hz, $CH^{Ph\text{-}ortho}$), 7.01 (t, 8H, $^3J_{HH}$ = 7 Hz, $CH^{BPh\text{-}ortho}$), 7.18 (t, 12H, $^3J_{HH}$ = 7 Hz, $CH^{Ph\text{-}para}$), 7.34 (m, 32H, overlapping $CH^{Ph\text{-}meta}$ and $CH^{BPh\text{-}meta}$). $^{13}C\{^1H\}$ NMR (CD_2Cl_2, 101 MHz) δ: 53.7 (s, CH_2), 122.2 (s, $CH^{BPh\text{-}para}$), 126.1 (s, $CH^{BPh\text{-}ortho}$), 128.0 (s, $CH^{Ph\text{-}ortho}$), 130.0 (s, $CH^{Ph\text{-}para}$), 133.8 (s, $CH^{Ph\text{-}meta}$), 136.5 (s, $CH^{BPh\text{-}meta}$). $^{31}P\{^1H\}$ NMR (CD_2Cl_2, 162 MHz) δ: 18.0 (s). HRMS (ES): m/z calcd. for $C_{78}H_{72}N_2P_6Cl_3{}^{101}Ru^{104}Ru$ ($[M - BPh_4]^+$) 1532.1297, found 1532.1685. Anal. Calcd for $C_{102}H_{92}BCl_3N_2P_6Ru_2$ (found): C, 62.83 (62.95); H, 4.85 (4.74); N, 1.42 (1.59).

NMR-Scale Reaction of $[Ru(NCMe)_3\{N(CH_2PPh_2)_3\text{-}\kappa^3P\}][PF_6]_2$ (12) and H_2. To a high-pressure NMR tube was added $[Ru(NCMe)_3\{N(CH_2PPh_2)_3\text{-}\kappa^3P\}][PF_6]_2$ (22.5 mg, 0.020 mmol) and partially dissolved in CD_2Cl_2 (0.5 mL) using a vortex stirrer. Initial ^{1}H, $^{31}P\{^1H\}$, and ^{19}F NMR analyses were carried out. The atmosphere in the NMR tube was changed to hydrogen by repeatedly evacuating and backfilling (×3) while the solution was frozen in liquid nitrogen, before the NMR tube was pressurized to 4 bar and allowed to warm to room temperature. The solution was analyzed by ^{1}H, $^{31}P\{^1H\}$, and ^{19}F NMR spectroscopy periodically for 6 days at room temperature and 7 days at 50 °C. Almost no reactivity was observed.

NMR-Scale Reaction of $[Ru(NCMe)_3\{N(CH_2PPh_2)_3\text{-}\kappa^3P\}][PF_6]_2$ (12) and Levulinic Acid. To a Young's tap NMR tube was added $[Ru(NCMe)_3\{N(CH_2PPh_2)_3\text{-}\kappa^3P\}][PF_6]_2$ (24.6 mg, 0.022 mmol) and partially dissolved in CD_2Cl_2 (0.6 mL) using a vortex stirrer. Initial ^{1}H, $^{31}P\{^1H\}$, and ^{19}F NMR analyses were carried out. A solution of levulinic acid (5.3 mg) in CD_2Cl_2 (0.3 mL) was prepared in a separate Schlenk flask, and 0.22 mL (3.9 mg levulinic acid, 0.034 mmol, 1.5 equiv) was added to the solution of **12** via syringe at room temperature. The solution was analyzed by ^{1}H, $^{31}P\{^1H\}$, and ^{19}F NMR spectroscopy periodically for 9 days at room temperature and 7 days at 50 °C. Almost no reactivity was observed.

■ ASSOCIATED CONTENT

Ⓢ Supporting Information

The following file is available free of charge on the ACS Publications website at DOI: 10.1021/cs502025t.

Gas chromatograms of representative catalytic runs; tables detailing additional catalytic runs including mercury poisoning experiments; $^{31}P\{^1H\}$ NMR spectra of complexes **8**, **10**, and **13**; ^{1}H and $^{31}P\{^1H\}$ NMR spectra of complexes **14**−**16**. Additional crystallographic data, including 50% probability ellipsoid ORTEP diagram of **14-B**. Preliminary DFT studies (PDF)

■ AUTHOR INFORMATION

Corresponding Authors

*E-mail: n.long@imperial.ac.uk.

*E-mail: philip.miller@imperial.ac.uk.

Notes

The authors declare no competing financial interest.

■ ACKNOWLEDGMENTS

We thank Imperial College London for funding, via the Frankland Chair endowment. Johson Matthey plc are also thanked for the loan of the precious-metal salts used in this work. We are also grateful to Imperial College/EPSRC for a small equipment grant that enabled the purchase of high-pressure equipment.

■ REFERENCES

(1) (a) Huber, G. W.; Iborra, S.; Corma, A. *Chem. Rev.* **2006**, *106*, 4044−4098. (b) Chheda, J. N.; Huber, G. W.; Dumesic, J. A. *Angew. Chem., Int. Ed.* **2007**, *46*, 7164−7183. (c) Corma, A.; Iborra, S.; Velty, A. *Chem. Rev.* **2007**, *107*, 2411−2502. (d) Marshall, A.-L.; Alaimo, P. J. *Chem.—Eur. J.* **2010**, *16*, 4970−4980. (e) Takagaki, A.; Nishimura, S.; Ebitani, K. *Catal. Surv. Asia* **2012**, *16*, 164−182.

(2) (a) Zakzeski, J.; Bruijnincx, P. C. A.; Jongerius, A. L.; Weckhuysen, B. M. *Chem. Rev.* **2010**, *110*, 3552−3599. (b) Pandey, M. P.; Kim, C. S. *Chem. Eng. Technol.* **2011**, *34*, 29−41.

(3) Hartwig, J. F.; Sergeev, A. G. *Science* **2011**, *332*, 439−443.

(4) vom Stein, T.; Weigand, T.; Merkens, C.; Klankermayer, J.; Leitner, W. *ChemCatChem* **2013**, *5*, 439−441.

(5) Balaraman, E.; Fogler, E.; Milstein, D. *Chem. Commun.* **2012**, *48*, 1111−1113.

(6) Du, X.-L.; Bi, Q.-Y.; Liu, Y.-M.; Cao, Y.; He, H.-Y.; Fan, K.-N. *Green Chem.* **2012**, *14*, 935−939.

(7) van Putten, R.-J.; van der Waal, J. C.; de Jong, E.; Rasrendra, C. B.; Heeres, H. J.; de Vries, J. G. *Chem. Rev.* **2013**, *113*, 1499−1597.

(8) Zhou, C.-H.; Xia, X.; Lin, C.-X.; Tong, D.-S.; Beltramini, J. *Chem. Soc. Rev.* **2011**, *40*, 5588−5617.

(9) (a) Wettstein, S. G.; Alonso, D. M.; Chong, Y.; Dumesic, J. A. *Energy Environ. Sci.* **2012**, *5*, 8199−8203. (b) Qi, L.; Mui, Y. F.; Lo, S. W.; Lui, M. Y.; Akien, G. R.; Horváth, I. *ACS Catal.* **2014**, *4*, 1470−1477.

DOI: 10.1021/cs502025t
ACS Catal. 2015, 5, 2500−2512

(10) (a) Assary, R. S.; Curtiss, L. A. *Chem. Phys. Lett.* **2012**, *541*, 21−26. (b) Tukacs, J. M.; Király, D.; Strádi, A.; Novodarszki, G.; Eke, Z.; Dibó, G.; Kégl, T.; Mika, L. T. *Green Chem.* **2012**, *14*, 2057−2065. (c) Michel, C.; Zaffran, J.; Ruppert, A. M.; Matras-Michalska, J.; Jędrzejczyk, M.; Grams, J.; Sautet, P. *Chem. Commun.* **2014**, *50*, 12450−12453. (d) Ding, D.; Wang, J.; Xi, J.; Liu, X.; Lu, G.; Wang, Y. *Green Chem.* **2014**, *16*, 3846−3853.
(11) Serrano-Ruiz, J. C.; West, R. M.; Dumesic, J. A. *Annu. Rev. Chem. Biomol. Eng.* **2010**, *1*, 79−100.
(12) Geilen, F. M. A.; Engendahl, B.; Harwardt, A.; Marquardt, W.; Klankermayer, J.; Leitner, W. *Angew. Chem., Int. Ed.* **2010**, *49*, 5510−5514.
(13) Pagliaro, M.; Ciriminna, R.; Kimura, H.; Rossi, M.; Pina, C. D. *Angew. Chem., Int. Ed.* **2007**, *46*, 4434−4440.
(14) Aycock, D. F. *Org. Process Res. Dev.* **2007**, *11*, 156−159.
(15) Pace, B.; Hoyos, P.; Fernández, M.; Sinisterra, J. V.; Alcántara, A. R. *Green Chem.* **2010**, *12*, 1380−1382.
(16) Pace, V.; Hoyos, P.; Castoldi, L.; de Maria, P. D.; Alcántara, A. R. *ChemSusChem* **2012**, *5*, 1369−1379.
(17) (a) Hanton, M. J.; Tin, S.; Boardman, B. J.; Miller, P. *J. Mol. Catal. A: Chem.* **2011**, *346*, 70−78. (b) vom Stein, T.; Meuresch, M.; Limper, D.; Schmitz, M.; Hölscher; Coetzee, J.; Cole-Hamilton, D. J.; Klankermayer, J.; Leitner, W. *J. Am. Chem. Soc.* **2014**, *136*, 13217−13225.
(18) Coetzee, J.; Dodds, D. L.; Klankermayer, J.; Brosinski, S.; Leitner, W.; Slawin, A. M. Z.; Cole-Hamilton, D. J. *Chem.—Eur. J.* **2013**, *19*, 11039−11050.
(19) Mellone, I.; Peruzzini, M.; Rosi, L.; Mellmann, D.; Junge, H.; Beller, M.; Gonsalvi, L. *Dalton Trans.* **2013**, *42*, 2495−2501.
(20) Savourey, S.; Lefèvre, G.; Berthet, J.-C.; Cantat, T. *Chem. Commun.* **2014**, *50*, 14033−14036.
(21) (a) Beydoun, K.; vom Stein, T.; Klankermayer, J.; Leitner, W. *Angew. Chem., Int. Ed.* **2013**, *52*, 9554−9557. (b) Beydoun, K.; Ghattas, G.; Thenert, K.; Klankermayer, J.; Leitner, W. *Angew. Chem., Int. Ed.* **2014**, *53*, 11010−11014.
(22) (a) Wesselbaum, S.; vom Stein, T.; Klankermayer, J.; Leitner, W. *Angew. Chem., Int. Ed.* **2012**, *51*, 7499−7502. (b) Wesselbaum, S.; Moha, V.; Meuresch, M.; Brosinski, S.; Thenert, K. M.; Kothe, J.; vom Stein, T.; Englert, U.; Hölscher, M.; Klankermayer, J.; Leitner, W. *Chem. Sci.* **2015**, *6*, 693−704.
(23) Savourey, S.; Lefèvre; Berthet, J.-C.; Thuéry, P.; Genre, C.; Cantat, T. *Angew. Chem., Int. Ed.* **2014**, *53*, 10466−10470.
(24) Geilen, F. M. A.; Engendahl, B.; Hölscher, M.; Klankermayer, J.; Leitner, W. *J. Am. Chem. Soc.* **2011**, *133*, 14349−14358.
(25) Märkl, G.; Jin, G. Y. *Tetrahedron Lett.* **1981**, *22*, 1105−1108.
(26) Miller, P. W.; White, A. J. P. *J. Organomet. Chem.* **2010**, *695*, 1138−1145.
(27) Fillol, J. L.; Kruckenberg, A.; Scherl, P.; Wadepohl, H.; Gade, L. H. *Chem.—Eur. J.* **2011**, *17*, 14047−14062.
(28) Scherl, P.; Kruckenbery, A.; Mader, S.; Wadepohl, H.; Gade, L. H. *Organometallics* **2012**, *31*, 7024−7027.
(29) Phanopoulos, A.; Brown, N. J.; White, A. J. P.; Long, N. J.; Miller, P. W. *Inorg. Chem.* **2014**, *53*, 3742−3752.
(30) Rhodes, L. F.; Venanzi, L. M. *Inorg. Chem.* **1987**, *26*, 2692−2695.
(31) Bakhmutov, V. L.; Bakmutova, E. V.; Belkova, N. V.; Bianchini, C.; Epstein, L. M.; Masi, D.; Peruzzini, M.; Shubina, E. S.; Voronstov, E. V.; Zanobini, F. *Can. J. Chem.* **2001**, *79*, 479−489.
(32) (a) Widegren, J. A.; Finke, F. G. *J. Mol. Catal. A: Chem.* **2003**, *198*, 317−341. (b) Whitesides, G. M.; Hackett, M.; Brainard, R. L.; Lavalleye, J.-P. P. M.; Sowinski, A. F.; Izumi, A. N.; Moore, S. S.; Brown, D. W.; Staudt, E. M. *Organometallics* **1985**, *4*, 1819−1830.
(33) Walter, O.; Huttner, G.; Kern, R. *Z. Naturforsch.* **1996**, *51b*, 922−928.
(34) (a) Landgrafe, C.; Sheldrick, W. S.; Südfeld, M. *Eur. J. Inorg. Chem.* **1998**, 407−414. (b) Bianchini, C.; Dal Santo, V.; Meli, A.; Oberhauser, W.; Psaro, R.; Vizza, F. *Organometallics* **2000**, *19*, 2433−2444.
(35) Bratsos, J.; Alessio, E. *Inorg. Synth.* **2010**, *35*, 148−152.

DOI: 10.1021/cs502025t
ACS Catal. 2015, 5, 2500−2512